The Journal of Neuroscience, April 15, 1996, 16(8):2671–2683

Dual Somatotopical Representations in the Primate Subthalamic Nucleus: Evidence for Ordered but Reversed Body-Map Transformations from the Primary Motor Cortex and the Supplementary Motor Area

Atsushi Nambu,[1] Masahiko Takada,[2] Masahiko Inase,[1] and Hironobu Tokuno[2]

[1]National Institute for Physiological Sciences, Okazaki 444, Japan, and [2]Department of Morphological Brain Science, Faculty of Medicine, Kyoto University, Kyoto 606-01, Japan

The subthalamic nucleus (STN) is a key structure for somatic motor control via the basal ganglia. In the present study, we demonstrate that the STN of the macaque monkey has dual sets of body part representations. Each of the two separate portions of the STN is characterized with somatotopically arranged direct cortical inputs that are derived from the primary motor cortex (MI) and the supplementary motor area (SMA). The first set of body part representations is transformed from the MI to the lateral STN, whereas the second set is transformed from the SMA to the medial STN.

Intracortical microstimulation mapping was carried out to guide paired injections of anterograde tracers into somatotopically corresponding regions of the MI and the SMA. We found that direct inputs from the MI were allocated mostly within the lateral half of the STN, whereas those from the SMA were distributed predominantly within its medial half. Of particular interest was that the arrangement of somatotopical representations from the SMA to the medial STN was reversed against the ordering of those from the MI to the lateral STN; the orofacial, forelimb, and hindlimb parts were represented from medial to lateral within the medial STN, whereas these body parts were represented, in the inverse order, mediolaterally within the lateral STN. Moreover, inputs from homotopical MI and SMA regions were found to converge only partially into the STN. The present findings could account for somatotopically specific involuntary movements manifested in hemiballism that is caused by destruction of the STN.

Key words: basal ganglia; subthalamic nucleus; primary motor cortex; supplementary motor area; body part representation; hemiballism

Because discrete lesions in the subthalamic nucleus (STN) result in a violent form of dyskinesia, termed "hemiballism," that is characterized by involuntary movements occurring in the contralateral limbs (Martin, 1927; Whittier, 1947; Whittier and Mettler, 1949; Carpenter et al., 1950; Carpenter and Carpenter, 1951; Carpenter and Mettler, 1951; Hamada and DeLong, 1992) (see also Crossman et al., 1980, 1984), the STN has long been recognized to play crucial roles in somatic motor control (for review, see Kitai and Kita, 1987; Albin et al., 1989; DeLong, 1990) (see also Bergman et al., 1990). It now seems a consensus that the STN may occupy the central position in an indirect pathway connecting the striatum to the output nuclei of the basal ganglia, the internal segment of the globus pallidus (GPi) and the substantia nigra pars reticulata (SNr), which is structurally parallel with, although functionally opposing to, a direct pathway to the GPi/SNr (Alexander et al., 1986, 1990; Alexander and Crutcher, 1990). Activation of striatal neurons tends to suppress the activity of neurons in the external segment of the globus pallidus (GPe) and thereby allow disinhibition of STN neurons, thus exerting an excitatory drive on GPi/SNr neurons. This, in turn, leads to increased inhibition of the thalamus and thalamocortical neurons.

In general, many pieces of somatic motor information from the primary motor cortex (MI) have been considered to be conveyed indirectly to the STN by way of the corticostriatal projections and the subsequent intrinsic (striatum–GPe–STN) relay of the basal ganglia (see Alexander and Crutcher, 1990; Alexander et al., 1990). In addition to this indirect route, the STN is likely to receive such information through the "hyperdirect" link (i.e., the direct cortico-STN pathway). By means of the autoradiographic tract-tracing technique, early anatomical work has shown that in the macaque monkey the STN receives somatotopically organized hyperdirect cortical inputs from the MI (Hartmann-von Monakow et al., 1978). Based on these MI inputs, somatotopical representations in the STN appeared to be arranged mediolaterally in the order of the hindlimb, forelimb, and orofacial part (Hartmann-von Monakow et al., 1978), although body part representations of the MI regions examined were not identified electrophysiologically. Despite the occurrence of somatotopically specific ballistic movements caused by varied extents of STN lesions, however, this body map was apparent only to the lateral portion of the STN, but not to its medial portion. In this context, there still exists an open question as to the somatotopy over the entire STN that reconciles with the somatotopical specificity of dyskinesias manifested in hemiballism (see DeLong et al., 1985; Wichmann et al., 1994).

In the present study, we therefore made an attempt to investi-

Received Nov. 1, 1995; revised Jan. 16, 1996; accepted Jan. 23, 1996.

This work was supported by joint research projects of the National Institute for Physiological Sciences. We thank J. Tanji for critical reading of this manuscript. We thank A. Uesugi and M.-L. Zhang for photographic help. We also thank M. Seo for technical assistance.

Correspondence should be addressed to Masahiko Takada, Department of Morphological Brain Science, Faculty of Medicine, Kyoto University, Yoshida-Konoe-cho, Sakyo-ku, Kyoto 606-01, Japan.

Dr. Nambu's present address: Department of Neurobiology, Tokyo Metropolitan Institute for Neuroscience, Fuchu, Tokyo 183, Japan.

Dr. Inase's present address: Molecular and Cellular Neuroscience Section, Electrotechnical Laboratory, Tsukuba 305, Japan.

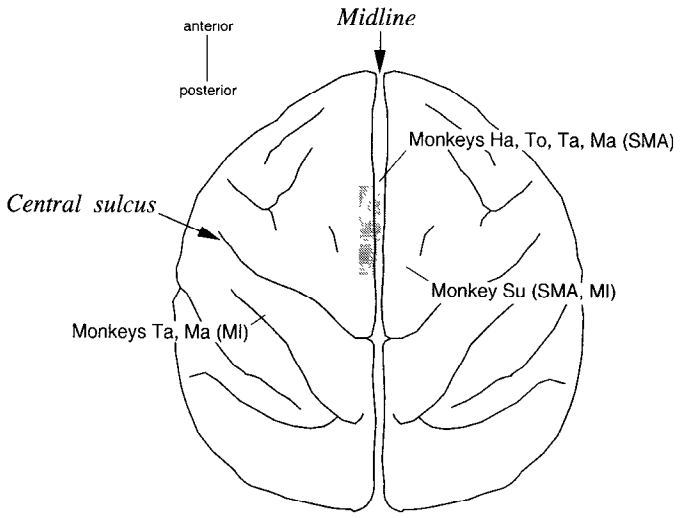

Figure 1. Schematic diagram showing the summary of the present experiments. Dorsal view of the monkey brain. Shown are the approximate locations of ICMS mapping and tracer injection in Monkeys *Ha*, *To*, *Su*, *Ta*, and *Ma*. See also Table 1 for details.

gate the somatotopical organization in the STN by analyzing the hyperdirect cortico-STN projections from the MI and the supplementary motor area (SMA)—the secondary motor cortex that is involved in many aspects of somatic motor behavior (for review, see Wiesendanger, 1986; Tanji, 1994)—in the macaque monkey. A series of experiments was designed to compare the distribution patterns in the STN of projection fibers from somatotopically corresponding regions of both cortical areas. To define MI and SMA regions representing various body parts, intracortical microstimulation (ICMS) was used in awake monkeys. Then double-anterograde axonal tracing was applied in single monkeys by injecting the distinguishable tracers wheat germ agglutinin-conjugated horseradish peroxidase (WGA-HRP) and biotinylated dextran amine (BDA) separately into electrophysiologically identified homotopical regions of the MI and the SMA.

MATERIALS AND METHODS

Five adult female Japanese monkeys (*Macaca fuscata*) were used for this study. Experiments were divided into two groups. The first group of experiments was designed for clarifying the somatotopical arrangement of the SMA–STN projections (Monkeys Ha, To, and Su-left), and the second group for comparing the SMA–STN and MI–STN projections (Monkeys Ta, Su-right, and Ma) (see Fig. 1, Table 1). This second group of experiments was to achieve the primary goal of the present study; paired injections of BDA and WGA-HRP were made into somatotopically corresponding regions of the SMA and the MI of the same hemisphere. Under general anesthesia, each monkey received surgical operation to gain easy access to electrophysiological mapping and subsequent tracer injections. All surgical procedures were done under aseptic conditions.

The monkeys were anesthetized with ketamine hydrochloride (10 mg/kg, i.m.) and sodium pentobarbital (30 mg/kg, i.m.) and positioned in a stereotaxic apparatus. The skull was widely exposed, and small, stainless steel screws were attached to the skull for anchor. The exposed skull and screws were completely covered with transparent acrylic resin. Two stainless steel pipes were mounted in parallel with each other over the frontal and occipital lobes for head fixation. A few days after the surgery, the monkeys were anesthetized with ketamine hydrochloride (10 mg/kg, i.m.) and xylazine hydrochloride (1–2 mg/kg, i.m.) and sat quietly in a primate chair with their heads fixed in a stereotaxic frame that was attached to the chair. Skull portions over the midline and/or the central sulcus were removed. After recovery from the anesthesia, each monkey underwent ICMS to determine physiologically the boundaries of body part representations in the SMA and/or the MI. Glass-insulated Elgiloy-

Table 1. Summary of experiments

	Site of tracer injection[a]	
Monkey	BDA	WGA-HRP
Ha (left)	SMA-forelimb (1 μl × 2)	
To (left)	SMA-forelimb (2 μl × 3)	SMA-hindlimb (0.1 μl × 1)
Su (left)		SMA-orofacial (0.1 μl × 1)
(right)	MI-hindlimb (1 μl × 6)	SMA-hindlimb (0.1 μl × 1)
Ta (left)	SMA-forelimb (1 μl × 2)	MI-forelimb (0.2 μl × 3)
Ma (left)	SMA-orofacial (2 μl × 2)	MI-orofacial (0.1 μl × 3)

See figures for further information about the cortical areas injected.

[a] The injection volume of each tracer and the number of needle penetrations are indicated in parentheses.

alloy microelectrodes, the impedance of which measured 0.9–1.4 MΩ at 500 Hz, were used for electrical stimulation as well as for recording of extracellular unit activity. Regions corresponding to the SMA and/or the MI were stimulated, via the electrode penetrated perpendicular to the cortical surface at 1000–1500 μm intervals, by currents ranging between 5 and 50 μA (22 or 12 cathodal pulses, respectively, for the SMA or the MI, 200 μsec duration at 333 Hz through a constant-current stimulator), and evoked movements of various body parts were observed. To verify the exact locations of the stimulation sites, electrolytic microlesions (anodal direct current of 10–15 μA, 20–30 sec) were placed at selected points before withdrawal of the electrode.

After ICMS mapping of the SMA and/or the MI, a single site or multiple sites were selected in each cortical area for injecting BDA (Molecular Probes, Eugene, OR; M_r 3000 kDa) (Fritzsch, 1993) or WGA-HRP (Toyobo; RZ ≥ 3.0) into one of the orofacial, forelimb, and hindlimb regions. Six different types of tracer injections were made as shown in Table 1. When paired deposits of BDA and WGA-HRP were placed in single monkeys (Monkeys To, Ta, Su-right, and Ma), the BDA injection was, in fact, carried out 10–18 d before the WGA-HRP injection. A total volume of 2–6 μl of a 20% solution of BDA dissolved in 0.01 M phosphate buffer, pH 7.3, was injected through a 10 μl Hamilton microsyringe that was attached to the same manipulator as the electrode, while a total volume of 0.1–0.6 μl of a 4% solution of WGA-HRP in 0.1 M Tris-HCl buffer, pH 7.0, was injected through a 1 μl Hamilton microsyringe in the same manner as used for BDA injection.

After a survival period of 14–21 d for BDA and 3–4 d for WGA-HRP, the monkeys were anesthetized deeply with an overdose of sodium pentobarbital (60 mg/kg, i.p.) and perfused transcardially with 0.1 M PBS, pH 7.3, followed by 8% formalin dissolved in 0.1 M PBS, pH 7.3 and, finally, the same fresh PBS containing 10% and then 30% sucrose. The brains were removed immediately, saturated with 30% sucrose in 0.1 M PBS, pH 7.3, at 4°C, and then cut serially into 60-μm-thick coronal sections on a freezing microtome. Every six sections were histochemically stained for BDA, and their adjacent ones for WGA-HRP. For visualizing injected and transported BDA, the sections were incubated in 0.05 M PBS, pH 7.3, containing 0.5% Triton X-100 overnight, followed by the same fresh PBS containing avidin–biotin–peroxidase complex (ABC Elite, Vector Laboratories, Burlingame, CA; 1:50 dilution) for 2 hr. This ABC incubation procedure was done after treatment of the sections with 1% H_2O_2 to eliminate cross-reaction with WGA-HRP and to inhibit endogenous peroxidases. The sections were then reacted for 10–20 min in 0.05 M Tris-HCl buffer, pH 7.6, containing 0.04% diaminobenzidine tetrahydrochloride, 0.04% $NiCl_2$ (Hancock, 1982), and 0.003% H_2O_2. For visualizing injected and transported WGA-HRP, the sections were reacted according to the tetramethylbenzidine (TMB) method (Mesulam, 1978) and incubated for 15 min in a 3% aqueous solution of ammonium molybdate to stabilize the reaction product (Fujii and Kusama, 1984). All sections were mounted onto gelatin-coated glass slides, counterstained with 1% Neutral Red, and then coverslipped.

Injection sites were charted in the coronal sections with the aid of a profile projector and reconstructed on the electrophysiological map as viewed from the cortical surface. Patterns of anterograde labeling in the STN were analyzed with the aid of both a profile projector and a camera lucida attached to a light microscope; adjacent sections were carefully aligned taking into account the greater shrinkage of the TMB-reacted sections. Parts of data concerning anterograde labeling in other brain structures than the STN were reported separately (Tokuno et al., 1995a,b).

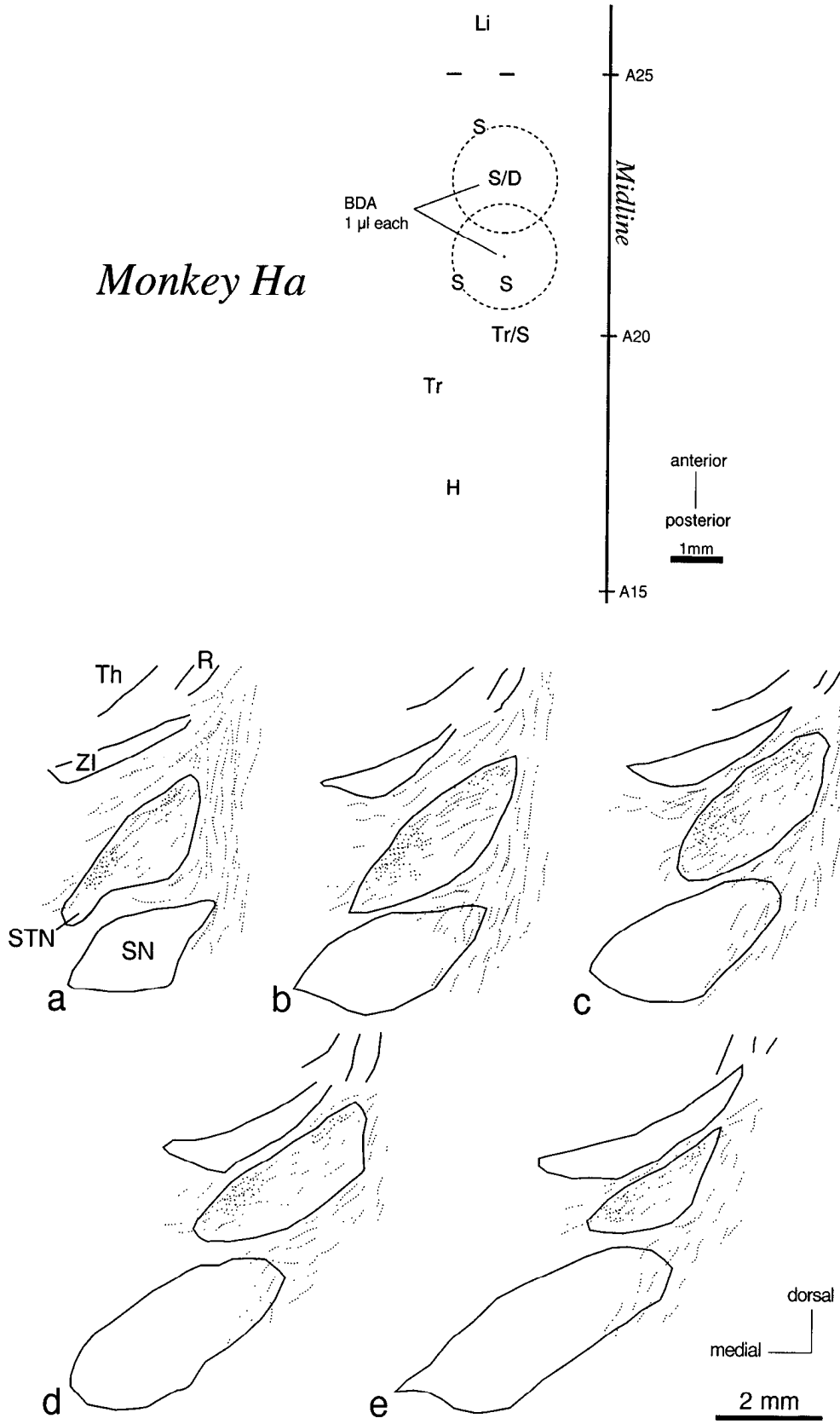

Figure 2. *Top*, ICMS mapping of the SMA in Monkey Ha and the sites of *BDA* injection in its forelimb region. Each letter represents the site of electrode penetration, stimulation of which elicited movement predominantly from one of the following body parts: lip (*Li*), digit (*D*), shoulder (*S*), trunk (*Tr*), and hip (*H*). –, No movement elicited. *Broken circles* indicate the approximate extents of tracer deposits. *Bottom*, Pattern of distribution of anterogradely labeled axon terminals (*dots*) and fibers of passage (*dotted lines*) in the *STN* and its surroundings. Five equidistant coronal sections through the STN are arranged rostrocaudally in *a–e*. *R*, Thalamic reticular nucleus; *SN*, substantia nigra; *Th*, thalamus; *ZI*, zona incerta.

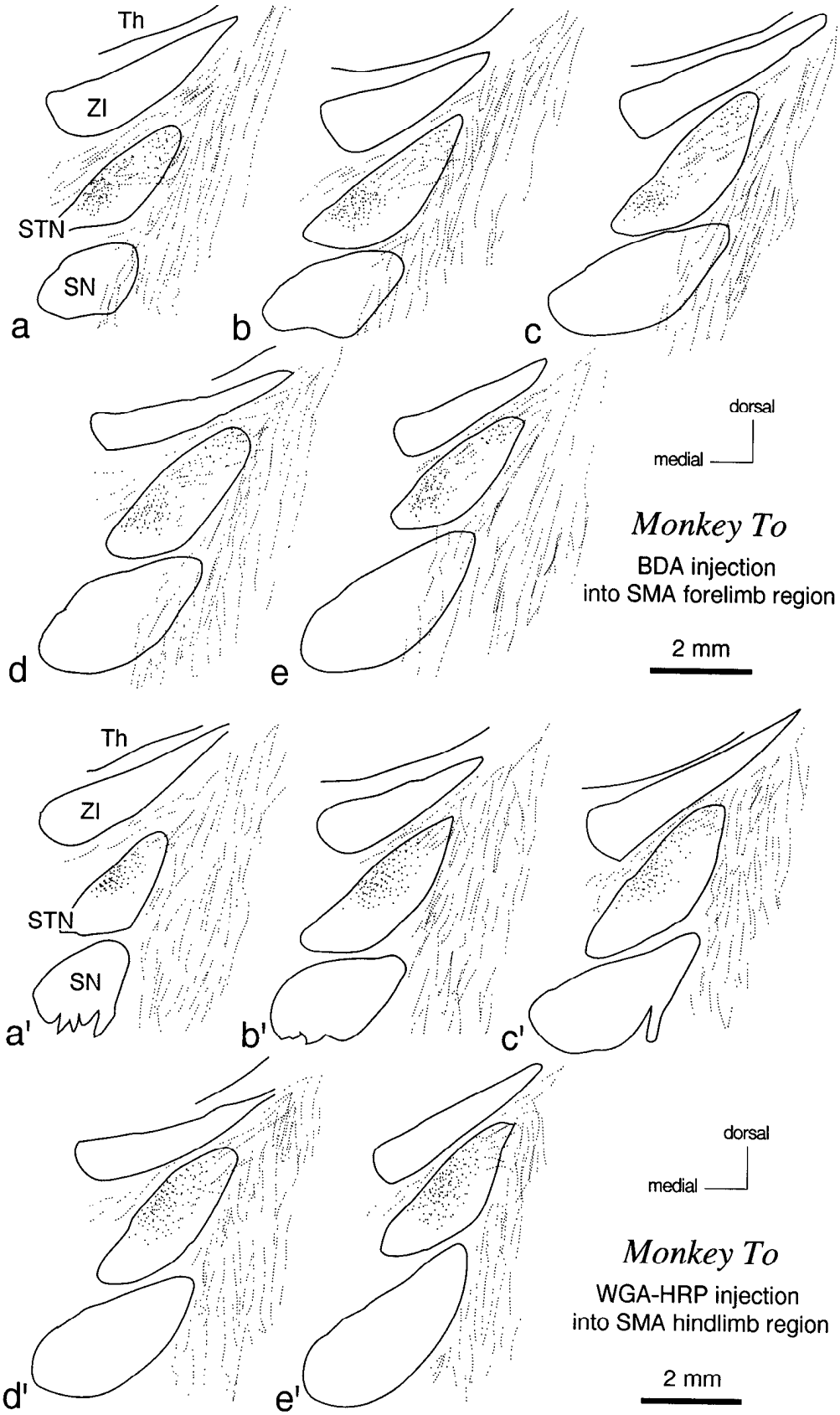

Figure 3. Patterns of distribution of anterogradely labeled axon terminals (*dots*) and fibers of passage (*dotted lines*) in the *STN* and its surroundings in Monkey To. For BDA labeling from the SMA forelimb region, five equidistant coronal sections through the STN are arranged rostrocaudally in *a–e*, and for WGA-HRP labeling from the SMA hindlimb region, their adjacent sections (60 μm apart) are arranged rostrocaudally in *a'–e'*. *SN*, Substantia nigra; *Th*, thalamus; *ZI*, zona incerta.

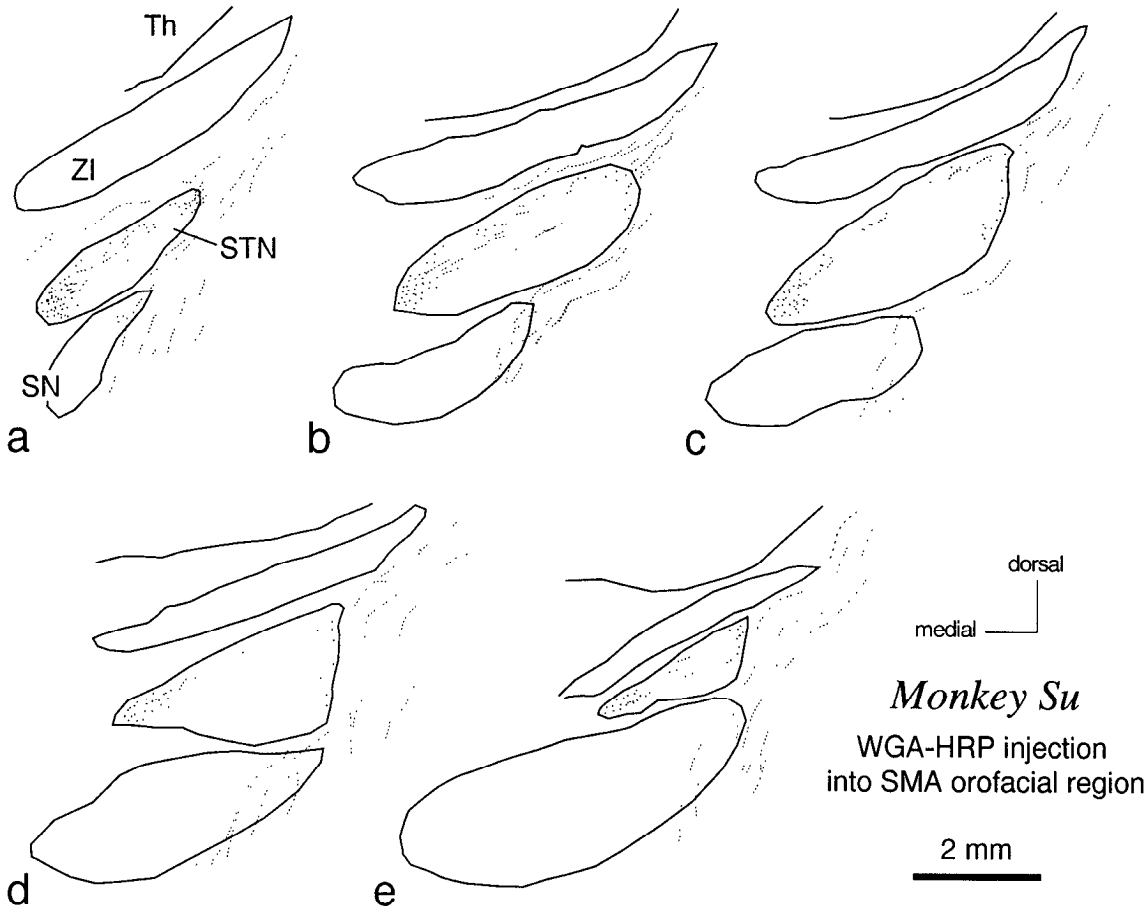

Figure 4. Pattern of distribution of anterogradely labeled axon terminals (*dots*) and fibers of passage (*dotted lines*) in the *STN* and its surroundings in Monkey Su. On this *left*, WGA-HRP was injected into the orofacial region of the SMA. Five equidistant coronal sections through the STN are arranged rostrocaudally in *a–e*. *SN*, Substantia nigra; *Th*, thalamus; *ZI*, zona incerta.

RESULTS

Throughout the experiments, results from ICMS mapping of the SMA and the MI were in accordance with the previously reported pattern of body part representations in each cortical area (Sessle and Wiesendanger, 1982; Mitz and Wise, 1987; Luppino et al., 1991); the orofacial, forelimb, and hindlimb regions of the SMA were arranged from rostral to caudal along the medial wall of the hemisphere, and those of the MI were arranged from lateral to medial along the anterior bank of the central sulcus (Figs. 2, 5) (Tokuno et al., 1995a,b). Histological reconstruction of serial coronal sections through the frontal cortex confirmed that the injection sites of BDA and WGA-HRP were almost successfully localized to the electrophysiologically identified orofacial, forelimb, and hindlimb regions of the SMA and the MI. In Monkey To, which was injected with WGA-HRP into the SMA hindlimb region, and in Monkey Su-right, which was injected with WGA-HRP and BDA into the SMA and MI hindlimb region, respectively, the boundary between the SMA (Brodmann's area 6) and the MI (Brodmann's area 4) was roughly determined based on the following previously described cytoarchitectonic and physiological criteria (Wise and Tanji, 1981; Mitz and Wise, 1987; Luppino et al., 1991; Matelli et al., 1991): (1) changes in density and distribution of giant layer V pyramidal cells, (2) changes in cellularity and organization of layer III, and (3) changes in movement thresholds and characteristics. In these monkeys, no diffusion of either tracer was detected at all beyond the boundary.

Somatotopical arrangement of SMA inputs in the STN

In the first group of experiments, we examined the somatotopical arrangement of SMA inputs in the STN. In Monkey Ha, BDA deposits were placed in the SMA forelimb region (Figs. 2, 9). In Monkey To, paired deposits of BDA and WGA-HRP were placed in the SMA forelimb and hindlimb region of the same hemisphere, respectively. In Monkey Su-left, WGA-HRP deposits were placed in the SMA orofacial region. In these experiments, when a cluster of randomly oriented fine varicose axons was observed, it was considered to be an indication of terminal labeling.

In all three monkeys, substantial numbers of fibers and terminals anterogradely labeled with BDA and WGA-HRP were seen in the STN (Figs. 2–4). The anterograde labeling in the STN occurred on the side ipsilateral to each injection. Accumulations of terminal label were found predominantly within the medial half of the STN and additionally within its lateral half. Within the medial STN, the distribution areas of axon terminals labeled from the orofacial, forelimb, and hindlimb regions of the SMA were, in this order, arranged from medial to lateral (Figs. 2–4). The medial-most zone of the medial STN contained axon terminals labeled from the orofacial region (Monkey Su-left; Fig. 4),

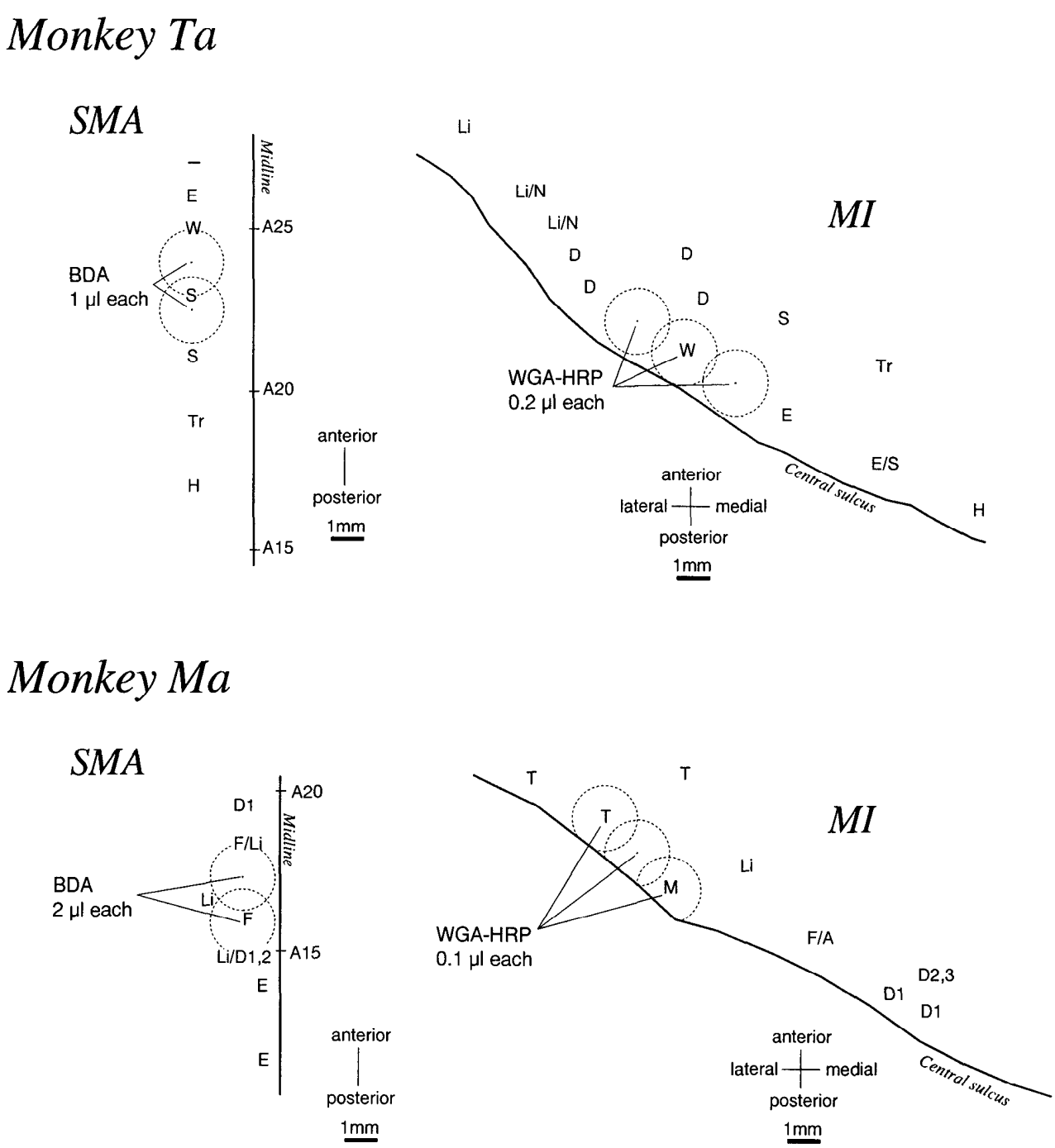

Figure 5. *Top*, ICMS mapping of the *SMA* and the *MI* in Monkey Ta, and the sites of paired injections of *BDA* and *WGA-HRP* in their forelimb regions. *Bottom*, ICMS mapping of the *SMA* and the *MI* in Monkey Ma, and the sites of paired injections of *BDA* and *WGA-HRP* in their orofacial regions. Each letter represents the site of electrode penetration, stimulation of which elicited movement predominantly from one of the following body parts: face (*F*), lip (*Li*), mouth (*M*), nose (*N*), tongue (*T*), arm (*A*), digit (*D*), wrist (*W*), elbow (*E*), shoulder (*S*), trunk (*Tr*), and hip (*H*). –, No movement elicited. *Broken circles* indicate the approximate extents of tracer deposits.

whereas the lateral-most zone of the medial STN contained those from the hindlimb region (Monkey To; Fig. 3). The terminal labeling from the forelimb region was located in between (Monkeys Ha and To; Figs. 2, 3). The areas of distribution of labeled axon terminals within the lateral STN were also found separate mediolaterally from case to case. However, their arrangement was totally opposite to that obtained for the medial STN; accumulations of terminal label from the orofacial, forelimb, and hindlimb regions of the SMA were, in this order, shifted from lateral to medial within the lateral STN (Figs. 2–4).

As far as the terminal labeling from the SMA hindlimb and forelimb regions was concerned, no extensive overlap was observed between the distribution area of each (Monkey To; Fig. 3). Similarly, the distribution areas of axon terminals labeled from the SMA forelimb and orofacial regions appeared to overlap to a minimal extent (compare Monkeys Ha/To and Su-left in Figs.

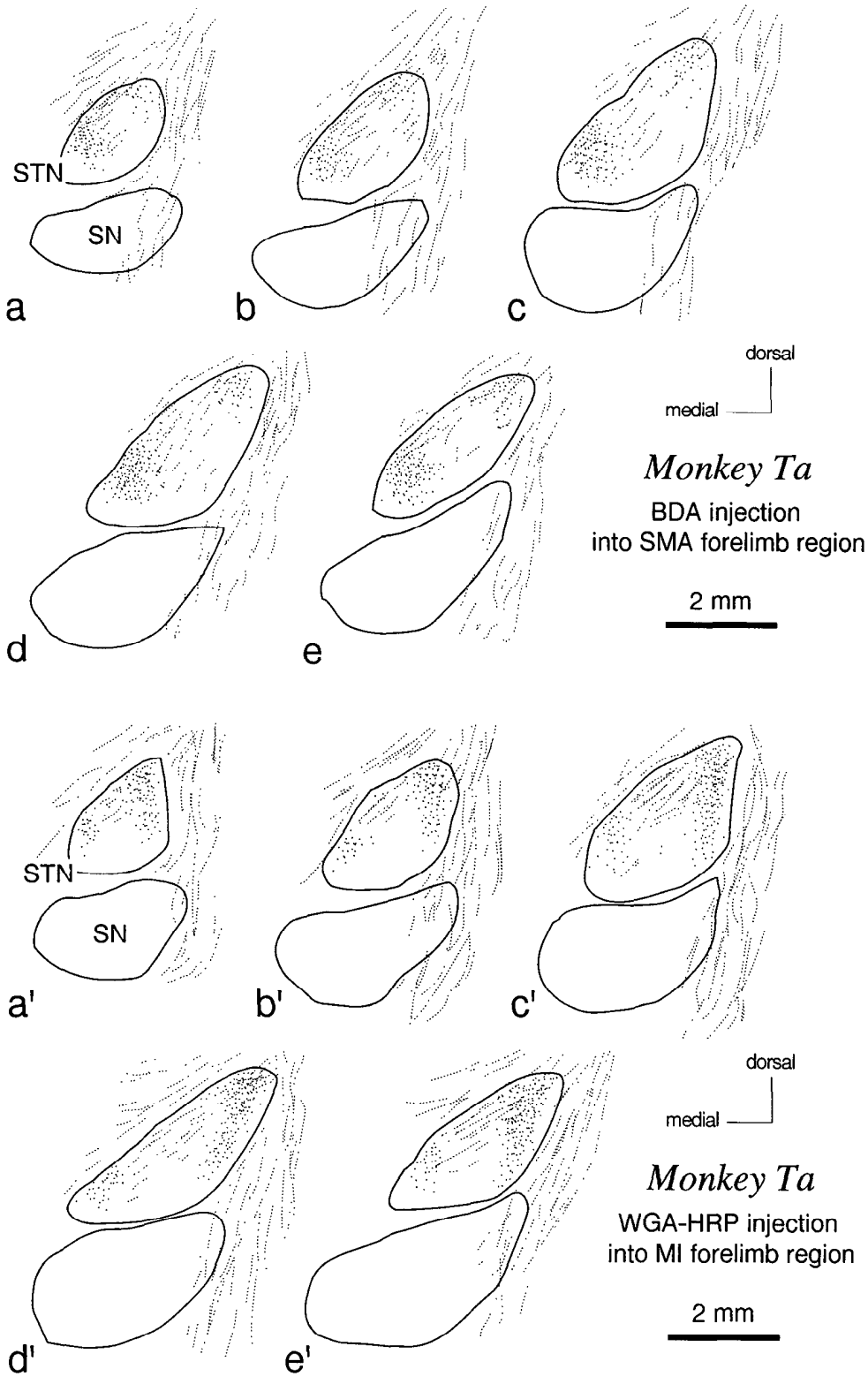

Figure 6. Patterns of distribution of anterogradely labeled axon terminals (*dots*) and fibers of passage (*dotted lines*) in the *STN* and its surroundings in Monkey Ta. For BDA labeling from the SMA forelimb region, five equidistant coronal sections through the STN are arranged rostrocaudally in *a–e*, and for WGA-HRP labeling from the MI forelimb region, their adjacent sections (60 μm apart) are arranged rostrocaudally in *a'–e'*. *SN*, Substantia nigra.

2–4). No clear rostrocaudal topography in terminal labeling was observed in the STN throughout the experiments.

Differential somatotopical arrangement of SMA versus MI inputs in the STN

In the second group of experiments, we compared the distribution patterns of homotopical SMA and MI inputs in the STN. One tracer was injected into an SMA region representing one of the orofacial, forelimb, and hindlimb parts, and the other was injected into an MI region on the ipsilateral side that displays the corresponding body part representation. In Monkey Ta, paired deposits of BDA and WGA-HRP were placed in the SMA and MI forelimb region, respectively (Fig. 5). In Monkey Su-right, paired

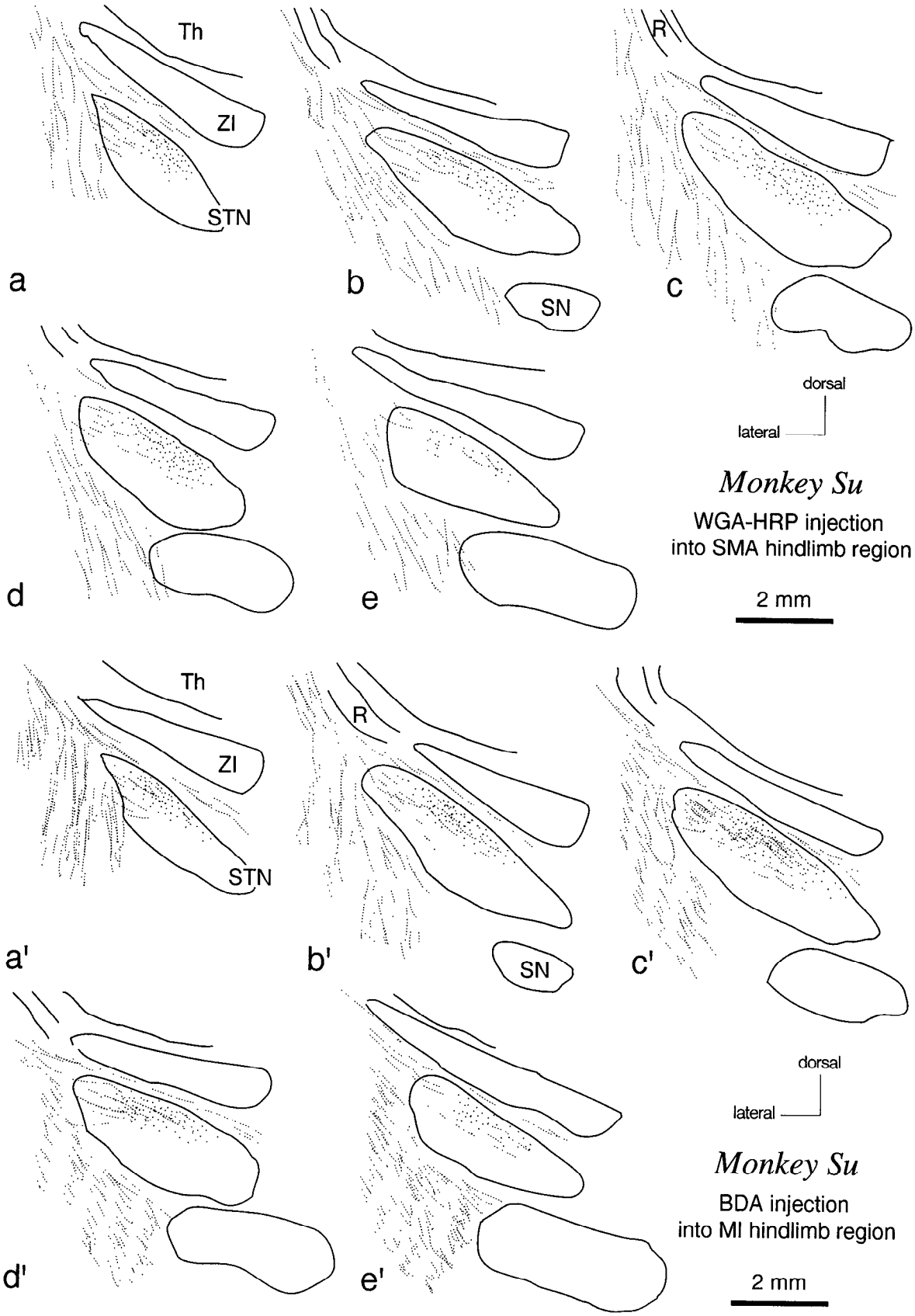

Figure 7. Patterns of distribution of anterogradely labeled axon terminals (*dots*) and fibers of passage (*dotted lines*) in the *STN* and its surroundings in Monkey Su. On this *right*, paired injections of WGA-HRP and BDA were made into the hindlimb regions of the SMA and the MI. For WGA-HRP labeling from the SMA hindlimb region, five equidistant coronal sections through the STN are arranged rostrocaudally in *a–e*, and for BDA labeling from the MI hindlimb region, their adjacent sections (60 μm apart) are arranged rostrocaudally in *a′–e′*. *R*, Thalamic reticular nucleus; *SN*, substantia nigra; *Th*, thalamus; *ZI*, zona incerta.

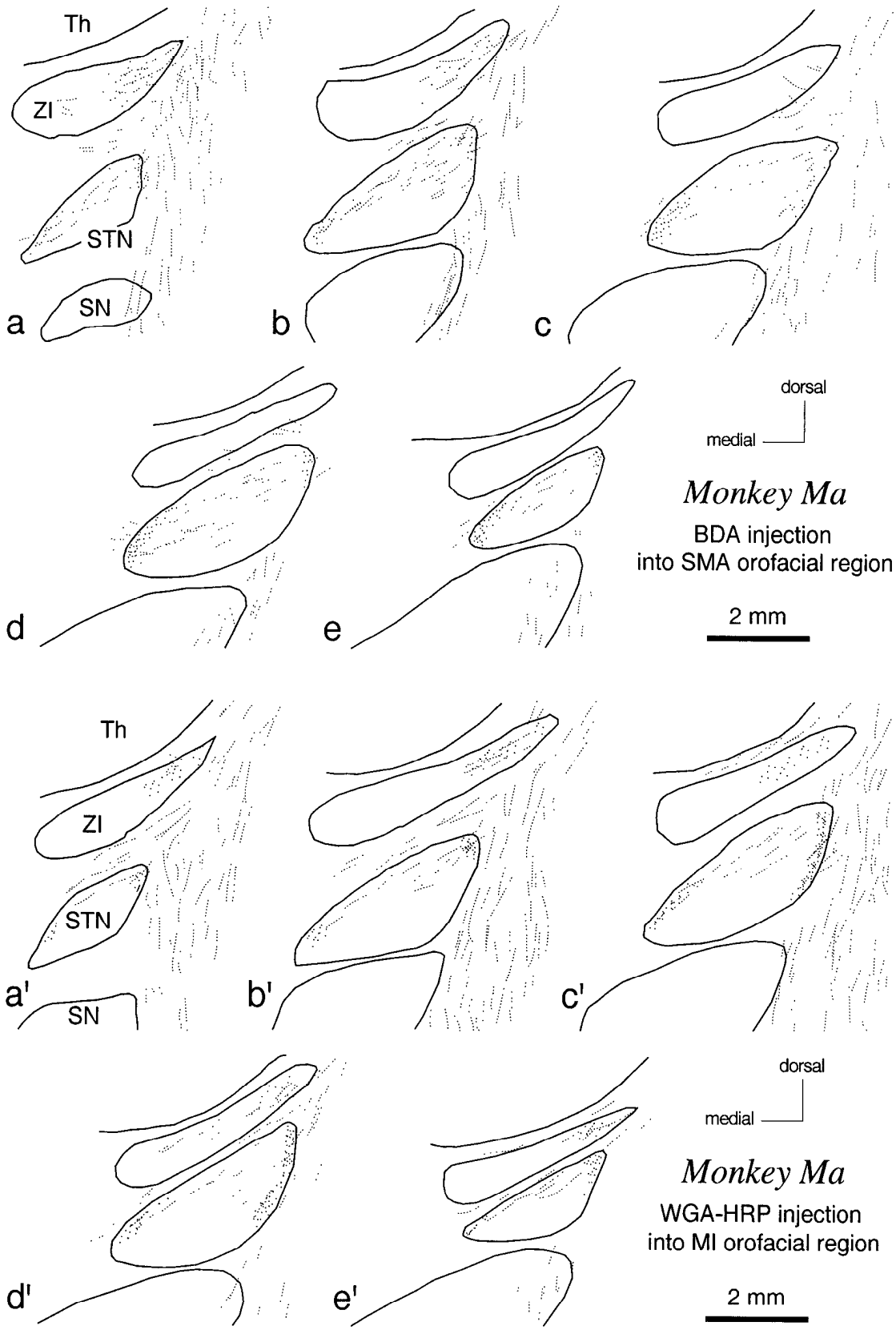

Figure 8. Patterns of distribution of anterogradely labeled axon terminals (*dots*) and fibers of passage (*dotted lines*) in the *STN* and its surroundings in Monkey Ma. For BDA labeling from the SMA orofacial region, five equidistant coronal sections through the STN are arranged rostrocaudally in *a–e*, and for WGA-HRP labeling from the MI orofacial region, their adjacent sections (60 μm apart) are arranged rostrocaudally in *a'–e'*. *SN*, Substantia nigra; *Th*, thalamus; *ZI*, zona incerta.

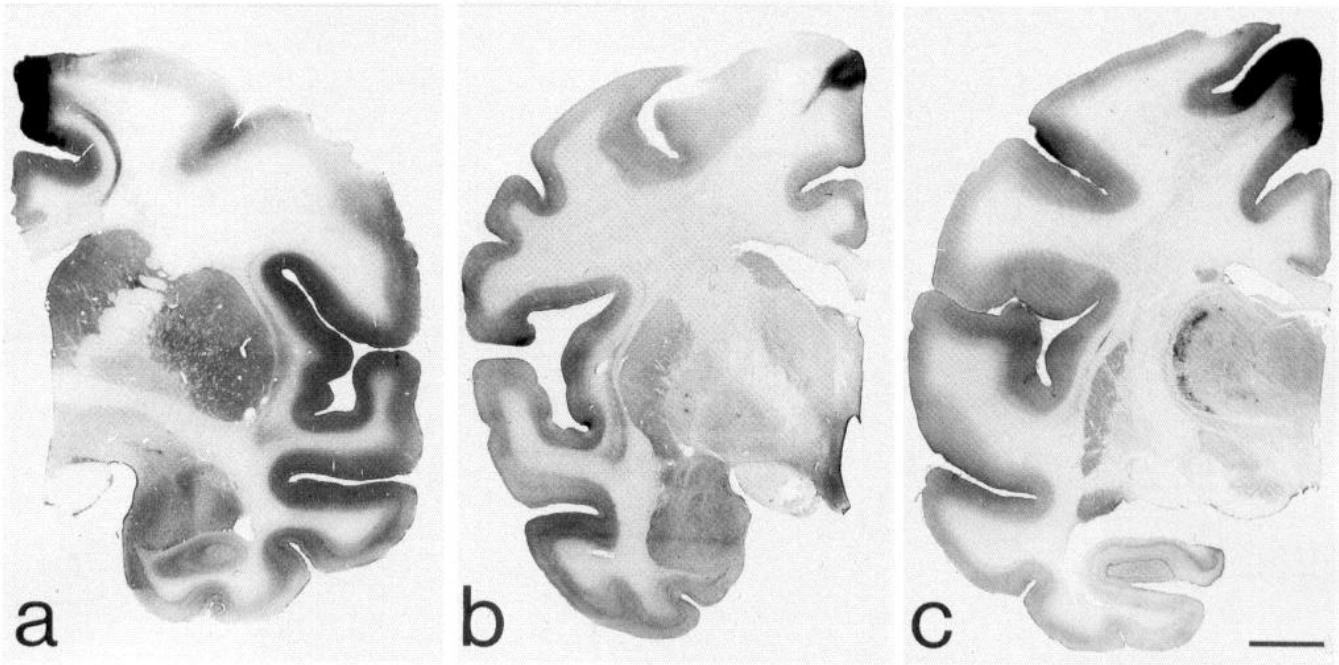

Figure 9. Examples of tracer injection sites in the SMA and the MI. *a*, Site of BDA injection in the SMA forelimb region in Monkey Ha. *b*, Site of WGA-HRP injection in the SMA hindlimb region in Monkey Su. *c*, Site of BDA injection in the MI hindlimb region in Monkey Su. Scale bar, 5 mm.

deposits of BDA and WGA-HRP were placed in the MI and SMA hindlimb region, respectively (Fig. 9). In Monkey Ma, paired deposits of BDA and WGA-HRP were placed in the SMA and MI orofacial region, respectively (Fig. 5).

In these monkeys, the distribution patterns in the STN of axon terminals labeled from SMA regions were essentially the same as described above. The terminal labeling occurred ipsilaterally and was more marked within the medial half than within the lateral half of the STN (Figs. 6–8). The areas of distribution of axon terminals labeled from the orofacial, forelimb, and hindlimb regions were arranged from medial to lateral within the medial STN (Fig. 10), whereas they were arranged in the inverse direction within the lateral STN. After injecting BDA or WGA-HRP into MI regions, anterogradely labeled fibers and terminals in the STN were also found on the side ipsilateral to each injection, although denser than those seen after injecting BDA or WGA-HRP into SMA regions (Figs. 6–8). Like the SMA-injection cases, accumulations of terminal label were observed simultaneously in two mediolaterally separate zones of the STN. In contrast to the SMA-injection cases, however, the dense accumulations were located within the lateral half of the STN (Fig. 10), whereas the sparse ones were located within its medial half. Within the lateral STN, the terminal labeling from the orofacial, forelimb, and hindlimb regions of the MI was evident in its lateral-most, central, or medial-most zone, respectively (Figs. 6–8). On the other hand, the arrangement of terminal label within the medial STN was totally opposite to that obtained for the lateral STN (Figs. 6–8). Again, no clear rostrocaudal topography in terminal labeling from either the SMA or the MI was detected in the STN throughout the experiments.

In each case of paired injections, careful alignment of serial series of adjacent sections (60 μm apart) stained for BDA and WGA-HRP revealed that the distribution areas of terminal label by the two independent tracers were in close register within both the medial and lateral STN (see Figs. 6–8). Throughout the experiments, virtually devoid of terminal labeling was the ventral portion of the STN, particularly in its mediolateral central zone.

DISCUSSION

The present findings have defined an anatomical substrate that dual sets of body part representations underlie the somatotopical organization in the primate STN (Fig. 11). Each of the two mediolaterally separate portions of the STN is characterized with somatotopically arranged hyperdirect cortical inputs from the MI and the SMA. The first set of body part representations is transformed mainly from the MI to the lateral STN, whereas the second set is transformed primarily from the SMA to the medial STN. In addition to these spatially segregated body map transformations, we have demonstrated a reversal of the ordered body part representations within the STN that are transformed through the hyperdirect MI and SMA projections. As also previously described (Hartmann-von Monakow et al., 1978) (see also DeLong et al., 1985; Wichmann et al., 1994), somatotopical representations in the lateral STN ("MI domain") are arranged from medial to lateral in the order of the hindlimb, forelimb, and orofacial part. By contrast, these body parts in the medial STN ("SMA domain") are represented mediolaterally in the inverse order, as if they were reflecting a "mirror image" against the somatotopical arrangement in the MI domain (Fig. 11). Such a reversed image of dual sets of body part representations in the STN may be compatible with the reported distribution of STN neurons responding to active movements and passive manipulations of individual body parts, as well as to somatosensory stimuli on them; clusters of STN neurons responsible for the hindlimb part, which lie centrally in the mediolateral dimension of the nucleus, tend to be sandwiched in between those responsible for the other body parts, including the forelimb and orofacial parts (DeLong et al., 1985; Wichmann et al., 1994). It has also been shown in the present study that virtually no inputs from either the MI or the SMA terminate in the ventral aspect of the STN,

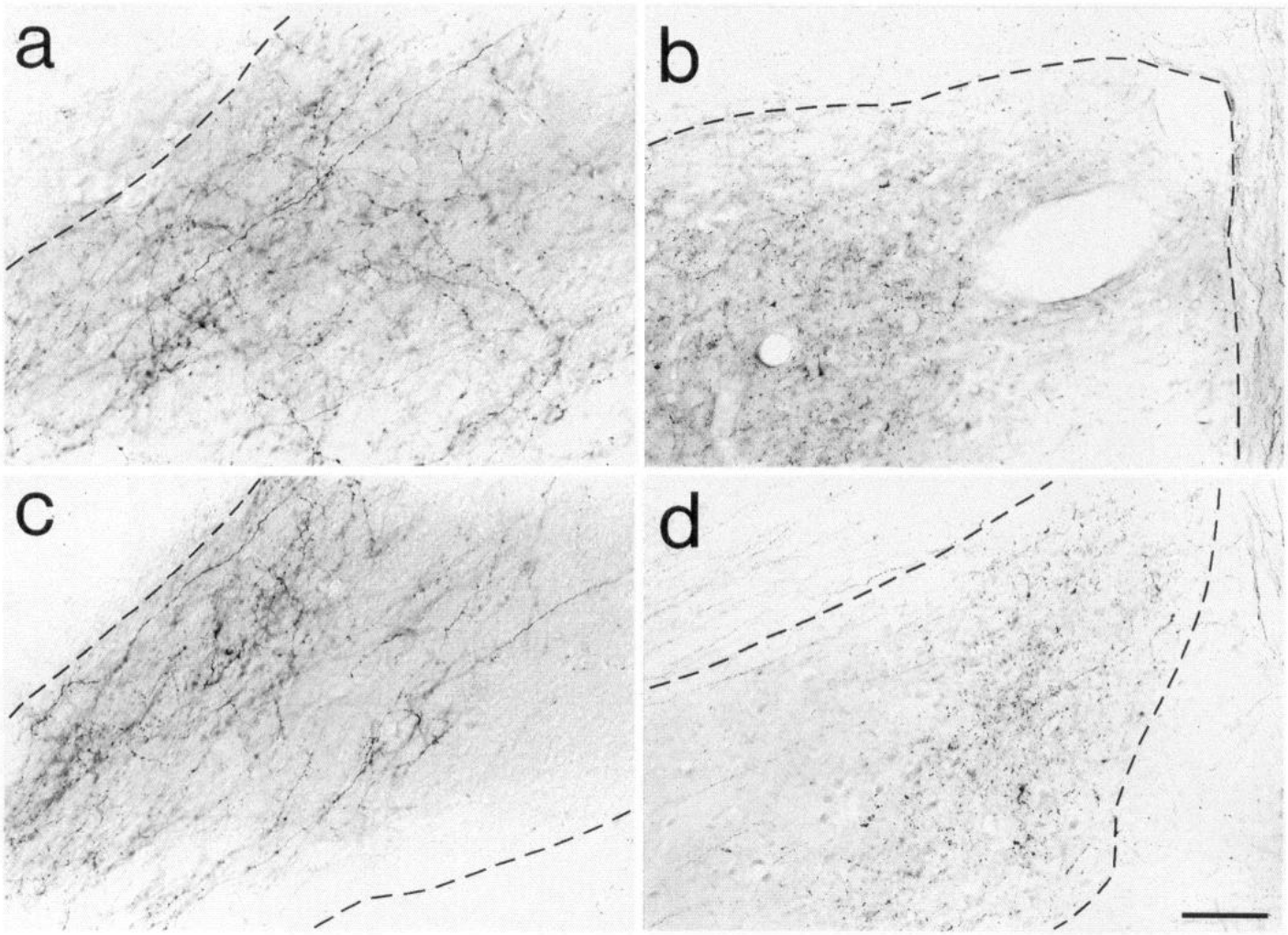

Figure 10. Examples of anterograde labeling in the STN. *a*, Anterograde labeling in the medial STN after BDA injection into the SMA forelimb region in Monkey Ta. *b*, Anterograde labeling in the lateral STN after WGA-HRP injection into the MI forelimb region in Monkey Ta. *c*, Anterograde labeling in the medial STN after BDA injection into the SMA orofacial region in Monkey Ma. *d*, Anterograde labeling in the lateral STN after WGA-HRP injection into the MI orofacial region in Monkey Ma. Scale bar, 40 μm.

particularly in its mediolateral central zone. This STN area has been reported to receive inputs from the frontal eye field and the supplementary eye field (Künzle and Akert, 1977; Hartmann-von Monakow et al., 1978; Huerta et al., 1986; Stanton et al., 1988; Huerta and Kaas, 1990; Shook et al., 1991) (see also Fig. 11) and has been implicated in the control of eye movements (Matsumura et al., 1992).

It seems a widely accepted theory of basal ganglia function that a parallel design is fundamental to information processing in pathways linking the basal ganglia and the frontal cortex (Alexander et al., 1986, 1990; Alexander and Crutcher, 1990). At least four loops—somatic motor, oculomotor, prefrontal, and limbic loops—so far have been differentiated for frontal cortex–basal ganglia circuits (Alexander and Crutcher, 1990; Alexander et al., 1990). Among current topics in basal ganglia research is the degree to which inputs from distinct, but functionally related, cortical areas converge within each circuit. There is a strong argument in favor of convergence of corticostriatal input systems within the oculomotor circuit; the distribution areas of striatal afferents from the frontal eye field and the supplementary eye field extensively overlap within the caudate nucleus (Parthasarathy et al., 1992). Another clear example of corticostriatal input convergence has been provided for the projections to the putamen from the primary somatosensory cortex and the MI (Flaherty and Graybiel, 1993) (see also Flaherty and Graybiel, 1991). In the present study, we have placed emphasis on parallel processing in the STN of signals derived from the MI and the SMA, both of which are principal cortical areas giving rise to the somatic motor circuit. It should also be mentioned here, however, that inputs from the MI and the SMA converge, albeit only partially, into the STN in a somatotopically matched manner (Fig. 11).

By analyzing the same monkey group as used in the present study, we have also found that corticostriatal inputs from homotopical MI and SMA regions of the same hemisphere are allocated to rather mediolaterally segregated zones of the putamen (Takada et al., 1995). Although both projections representing the hindlimb, forelimb, and orofacial parts are similarly arranged from dorsal to ventral within the putamen, their terminal fields are relatively differentially distributed such that projection fibers from the MI terminate more laterally, whereas those from the SMA terminate more medially. Interestingly, it seems likely that somatotopically corresponding regions of the STN and the striatum are interconnected with each other via subthalamostriatal projections. The dorsal portions of the STN project to the putamen for somatic motor function, whereas the more ventral ones project to the caudate nucleus for oculomotor function (see Smith

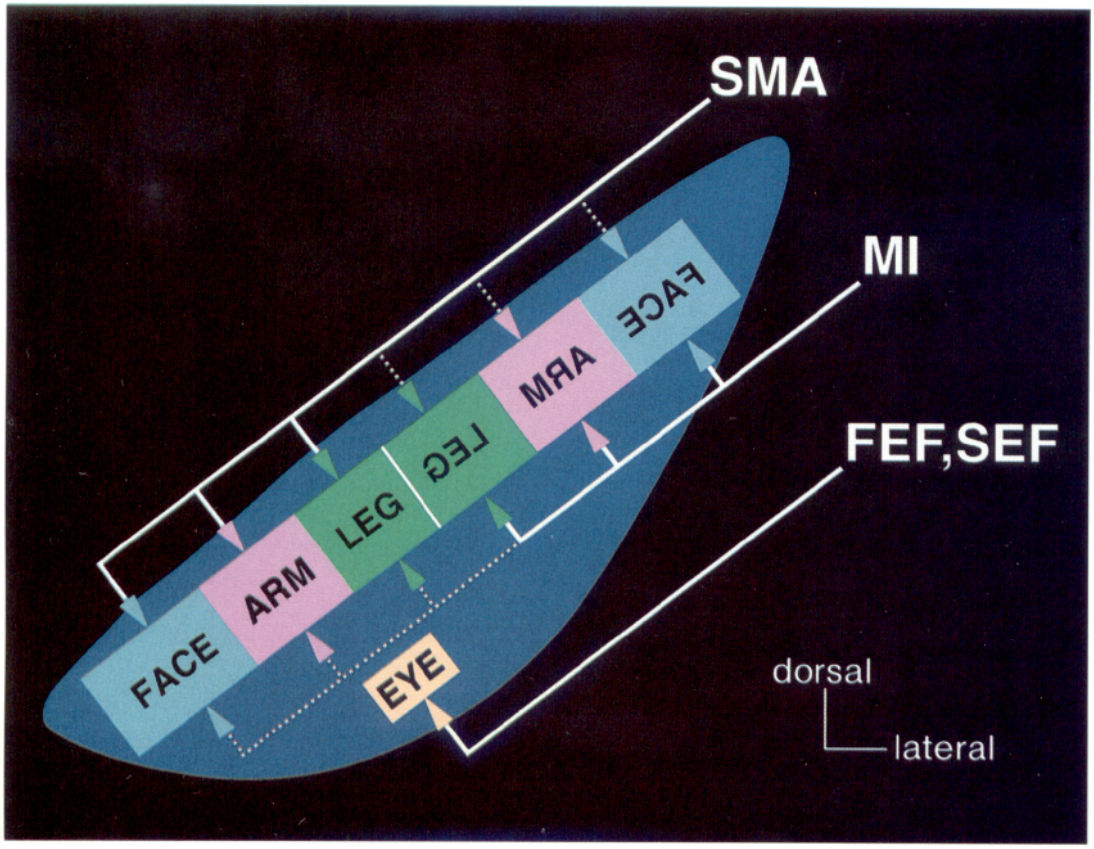

Figure 11. Summary diagram showing the "mirror image" organization of dual sets of somatotopical representations in the STN, as revealed by inputs from the *MI* and the *SMA*. *Dotted lines* indicate minor inputs. Note that inputs from the frontal (*FEF*) and supplementary (*SEF*) eye fields are confined to the ventral portion of the STN (Künzle and Akert, 1977; Hartmann-von Monakow et al., 1978; Huerta et al., 1986; Stanton et al., 1988; Huerta and Kaas, 1990; Shook et al., 1991).

and Parent, 1986; Parent and Smith, 1987; Nakano et al., 1990). At finer levels, the lateral-most and medial-most zones of the STN project to the ventral aspects of the putamen for orofacial movements, whereas the more central zones of the dorsal STN project to its dorsal aspects for forelimb and hindlimb movements (see Nakano et al., 1990). Such maintained somatotopy of the STN as well as of the putamen suggests that the somatic motor circuit may be composed of multiple parallel channels concerned with individual body parts or their specific movements.

The existence of the highly ordered somatotopical representations in the STN would help to elucidate how restricted lesions within the nucleus result in impaired movements of a single body part. No correlation in hemiballism has yet been revealed between the site of STN lesion and the somatotopical specificity of dyskinesia. It has been viewed, however, that dyskinesias experimentally produced by STN lesions bear the following characteristics (see Whittier and Mettler, 1949; Carpenter et al., 1950; Carpenter and Carpenter, 1951; Carpenter and Mettler, 1951; Hamada and DeLong, 1992): (1) the dyskinesias appear predominantly in the hindlimb and forelimb parts, but rarely in the orofacial part; (2) the hindlimb dyskinesias are more marked than the forelimb dyskinesias; and (3) the forelimb dyskinesias usually occur in association with the hindlimb dyskinesias. The reversed image of dual somatotopy in the STN that we have observed could account for these pathophysiological events in hemiballism. If the mediolateral central zone of the STN is destroyed, then the hindlimb zones of the MI and SMA domains are subject to simultaneous lesions. On the other hand, large lesions that infringe on a considerable part or on the entire mediolateral extent of the STN are perhaps required to destroy the forelimb and/or orofacial zones of both the MI and SMA domains. In particular, the orofacial zones of the MI and SMA domains are so remote as to be spared the simultaneous destruction; it should be noted here, however, that clinical reports have pointed out that orofacial dyskinesias appear when the oral pole of the STN is destroyed, and that they are often coupled with forelimb dyskinesias, but rarely with hindlimb ones (see Martin, 1927; Whittier, 1947; Carpenter and Carpenter, 1951). In such large-lesion cases, the hindlimb zones of the MI and SMA domains are constantly exposed to simultaneous lesions. It is conceivable, therefore, that a given body part may be affected more readily and severely when STN lesions encompass its homotopical zones of both the MI and SMA domains concurrently.

The following scheme should be provided for the participation of the hyperdirect cortico-STN pathways in somatic motor control via the basal ganglia (see also Kitai and Kita, 1987; Alexander and Crutcher, 1990; Alexander et al., 1990; DeLong, 1990). Activation of excitatory (putatively glutamatergic) STN neurons by hyperdirect cortical inputs from the MI and the SMA results in subsequent activation of neurons in the GPi and the SNr. This leads to suppression of thalamocortical circuits that is mediated through inhibitory pallidothalamic and nigrothalamic projections, thereby arresting movement. Thus, the hyperdirect pathways from the MI and the SMA to the STN could suppress movement more directly than the so called indirect striatal output pathway that has received so much attention.

REFERENCES

Albin RL, Young AB, Penney JB (1989) The functional anatomy of the basal ganglia disorders. Trends Neurosci 12:366–375.

Alexander GE, Crutcher MD (1990) Functional architecture of basal ganglia circuits: neural substrates of parallel processing. Trends Neurosci 13:266–271.

Alexander GE, DeLong MR, Strick PL (1986) Parallel organization of functionally segregated circuits linking basal ganglia and cortex. Annu Rev Neurosci 9:357–381.

Alexander GE, Crutcher MD, DeLong MR (1990) Basal ganglia-thalamocortical circuits: parallel substrates for motor, oculomotor, "prefrontal" and "limbic" functions. Prog Brain Res 85:119–146.

Bergman H, Wichmann T, DeLong MR (1990) Reversal of experimental parkinsonism by lesions of the subthalamic nucleus. Science 249:1436–1438.

Carpenter MB, Carpenter CS (1951) Analysis of somatotopic relations of the corpus Luysi in man and monkey. J Comp Neurol 95:349–370.

Carpenter MB, Mettler FA (1951) Analysis of subthalamic hyperkinesia in the monkey with special reference to ablations of agranular cortex. J Comp Neurol 95:125–158.

Carpenter MB, Whittier JR, Mettler FA (1950) Analysis of choreoid hyperkinesia in the rhesus monkey: surgical and pharmacological analysis of hyperkinesia resulting from lesions in the subthalamic nucleus of Luys. J Comp Neurol 92:293–332.

Crossman AR, Sambrook MA, Jackson A (1980) Experimental hemiballismus in the baboon produced by injection of a gamma-aminobutyric acid antagonist into the basal ganglia. Neurosci Lett 20:369–372.

Crossman AR, Sambrook MA, Jackson A (1984) Experimental hemichorea/hemiballismus in the monkey. Brain 107:579–596.

DeLong MR (1990) Primate models of movement disorders of basal ganglia origin. Trends Neurosci 13:281–285.

DeLong MR, Crutcher MD, Georgopoulos AP (1985) Primate globus pallidus and subthalamic nucleus: functional organization. J Neurophysiol 53:530–543.

Flaherty AW, Graybiel AM (1991) Corticostriatal transformations in the primate somatosensory system: projections from physiologically mapped body-part representations. J Neurophysiol 66:1249–1263.

Flaherty AW, Graybiel AM (1993) Two input systems for body representations in the primate striatal matrix: experimental evidence in the squirrel monkey. J Neurosci 13:1120–1137.

Fritzsch B (1993) Fast axonal diffusion of 3000 molecular weight dextran amines. J Neurosci Methods 50:95–103.

Fujii M, Kusama T (1984) Fixation of horseradish peroxidase reaction products with ammonium molybdate. Neurosci Res 1:153–156.

Hamada I, DeLong MR (1992) Excitotoxic acid lesions of the primate subthalamic nucleus result in transient dyskinesias of the contralateral limbs. J Neurophysiol 68:1850–1858.

Hancock MB (1982) DAB-nickel substrate for the differential immunoperoxidase staining of nerve fibers and terminals. J Histochem Cytochem 30:578.

Hartmann-von Monakow K, Akert K, Künzle H (1978) Projections of the precentral motor cortex and other cortical areas of the frontal lobe to the subthalamic nucleus in the monkey. Exp Brain Res 33:395–403.

Huerta MF, Kaas JH (1990) Supplementary eye field as defined by intracortical microstimulation: connections in macaques. J Comp Neurol 293:299–330.

Huerta MF, Krubitzer LA, Kaas JH (1986) Frontal eye field as defined by intracortical microstimulation in squirrel monkeys, owl monkeys, and macaque monkeys. I. Subcortical connections. J Comp Neurol 253:415–439.

Kitai ST, Kita H (1987) Anatomy and physiology of the subthalamic nucleus: a driving force of the basal ganglia. Adv Behav Biol 32:357–373.

Künzle H, Akert K (1977) Efferent connections of cortical, area 8 (frontal eye field) in *Macaca fascicularis*: a reinvestigation using the autoradiographic technique. J Comp Neurol 173:147–164.

Luppino G, Matelli M, Camarda RM, Gallese V, Rizzolatti G (1991) Multiple representations of body movements in mesial area 6 and the adjacent cingulate cortex: an intracortical microstimulation study in the macaque monkey. J Comp Neurol 311:463–482.

Martin JP (1927) Hemichorea resulting from a local lesion of the brain. (The syndrome of the body of Luys.) Brain 50:637–651.

Matelli M, Luppino G, Rizzolatti G (1991) Architecture of superior and mesial area 6 and the adjacent cingulate cortex in the macaque monkey. J Comp Neurol 311:445–462.

Matsumura M, Kojima J, Gardiner TW, Hikosaka O (1992) Visual and oculomotor functions of monkey subthalamic nucleus. J Neurophysiol 67:1615–1632.

Mesulam M-M (1978) Tetramethyl benzidine for horseradish peroxidase neurohistochemistry: a non-carcinogenic blue reaction product with superior sensitivity for visualizing neural afferents and efferents. J Histochem Cytochem 26:106–117.

Mitz AR, Wise SP (1987) The somatotopic organization of the supplementary motor area: intracortical microstimulation mapping. J Neurosci 7:1010–1021.

Nakano K, Hasegawa Y, Tokushige A, Nakagawa S, Kayahara T, Mizuno N (1990) Topographical projections from the thalamus, subthalamic nucleus and pedunculopontine tegmental nucleus to the striatum in the Japanese monkey, *Macaca fuscata*. Brain Res 537:54–68.

Parent A, Smith Y (1987) Organization of efferent projections of the subthalamic nucleus in the squirrel monkey as revealed by retrograde labeling methods. Brain Res 436:296–310.

Parthasarathy HB, Schall JD, Graybiel AM (1992) Distributed but convergent ordering of corticostriatal projections: analysis of the frontal eye field and the supplementary eye field in the macaque monkey. J Neurosci 12:4468–4488.

Sessle BJ, Wiesendanger M (1982) Structural and functional definition of the motor cortex in the monkey (*Macaca fascicularis*). J Physiol (Lond) 323:245–265.

Shook BL, Schlag-Rey M, Schlag J (1991) Primate supplementary eye field. II. Comparative aspects of connections with the thalamus, corpus striatum, and related forebrain nuclei. J Comp Neurol 307:562–583.

Smith Y, Parent A (1986) Differential connections of caudate nucleus and putamen in the squirrel monkey (*Saimiri sciureus*). Neuroscience 18:347–371.

Stanton GB, Goldberg ME, Bruce CJ (1988) Frontal eye field efferents in the macaque monkey. I. Subcortical pathways and topography of striatal and thalamic terminal fields. J Comp Neurol 271:473–492.

Takada M, Tokuno H, Nambu A, Inase M (1995) Somatotopical representations of inputs from the supplementary motor area in the putamen. Soc Neurosci Abstr 21:677.

Tanji J (1994) The supplementary motor area in the cerebral cortex. Neurosci Res 19:251–268.

Tokuno H, Takada M, Nambu A, Inase M (1995a) Somatotopical projections from the supplementary motor area to the red nucleus in the macaque monkey. Exp Brain Res 106:351–355.

Tokuno H, Takada M, Nambu A, Inase M (1995b) Direct projections from the orofacial region of the primary motor cortex to the superior colliculus in the macaque monkey. Brain Res 703:217–222.

Whittier JR (1947) Ballism and the subthalamic nucleus (nucleus hypothalamicus, corpus Luysi). Review of the literature and study of thirty cases. Arch Neurol Psychiatry 58:672–692.

Whittier JR, Mettler FA (1949) Studies on the subthalamus of the rhesus monkey. II. Hyperkinesia and other physiologic effects of subthalamic lesions, with special reference to the subthalamic nucleus of Luys. J Comp Neurol 90:319–372.

Wichmann T, Bergman H, DeLong MR (1994) The primate subthalamic nucleus. I. Functional properties in intact animals. J Neurophysiol 72:494–506.

Wiesendanger M (1986) Recent developments in studies of the supplementary motor area of primates. Rev Physiol Biochem Pharmacol 103:1–59.

Wise SP, Tanji J (1981) Supplementary and precentral motor cortex: contrast in responsiveness to peripheral input in the hindlimb area of the unanesthetized monkey. J Comp Neurol 195:433–451.